

SURFACE REFLECTANCE RETRIEVAL FROM AVIRIS DATA USING A SIX-DIMENSIONAL LOOK-UP TABLE

K. Staenz¹, D.J. Williams², and B. Walker²

¹Canada Centre for Remote Sensing
588 Booth Street, Ottawa, Ontario, Canada K1A 0Y7

²MacDonald Dettwiler and Associates Ltd.
13800 Commerce Parkway, Richmond, British Columbia, Canada V6V 2J3

1. INTRODUCTION

Surface reflectance retrieval has become important for quantitative information extraction and multi-temporal and multi-sensor data analysis. The trend related to surface reflectance retrieval in imaging spectrometry is the removal of atmospheric effects with radiative transfer codes in combination with the extraction of atmospheric parameters from the image data themselves (Staenz et al., 1994; Green et al., 1993; Gao et al., 1993; Carrère and Conel, 1992). Unfortunately, such procedures can be very demanding with respect to computation time, especially when data in the gaseous absorption regions are used for subsequent analysis. In order to reduce the run time of these procedures, a look-up table (LUT) based surface reflectance retrieval technique was developed on the Imaging Spectrometer Data Analysis System (ISDAS) (Staenz et al., 1996) of the Canada Centre for Remote Sensing. This paper presents an overview of the LUT generation and subsequent transfer of Airborne Visible/Infrared Imaging Spectrometer (AVIRIS) radiances into surface reflectances.

2. DATA SETS AND DATA PREPARATION

AVIRIS data used for this study were acquired over forested areas in rugged terrain near Canal Flats (scene 1) and near Victoria (scene 2), British Columbia in August of 1990 and 1993, respectively. Available ground reference information relevant to this study includes a digital elevation model (DEM) for scene 1 and reflectance measurements of various targets (asphalt, gravel, soccer field, etc.) and aerosol optical depth for scene 2.

The original DEM of 70 m grid size was resampled to the AVIRIS pixel size (20 m) and then registered to the image cube using the forest cover map. The registration with the nearest neighbour resampling technique resulted in a RMS error of ± 1.50 in the pixel direction and ± 0.95 in the line direction. The map-to-image registration has the advantage of maintaining the radiometric accuracy, which is important for surface reflectance retrieval. Due to the lack of a DEM for scene 2, only point calculations with respect to the retrieval of surface reflectance were carried out for specific targets with terrain elevations extracted from topographic maps.

3. SURFACE REFLECTANCE RETRIEVAL

3.1 Overview

Features of the surface reflectance retrieval procedure include the generation of a linear LUT to provide additive and multiplicative coefficients for removal of scattering and absorption effects, altitude-dependent layering of atmospheric gases and aerosols, scene-based estimation of atmospheric parameters such as water vapour, first-order removal of adjacency effects, Lambertian correction for slope and aspect effects, and choice of exo-atmospheric solar irradiance (E_0) functions from different sources in combination with the different radiative transfer (RT) codes. Available RT codes on ISDAS are M5S (modified version of 5S (Tanré et al., 1990) used at CCRS (Teillet and Santer, 1991)), LOWTRAN7 (Kneizys et al., 1988), or MODTRAN2 (Berk et al., 1989) and MODTRAN3 (Anderson et al., 1995). RT codes can easily be exchanged or added since they share the same user interface. The necessary parameters to run a specific RT code are then automatically extracted from the various input tables. This

surface reflectance retrieval procedure can be applied to individual spectra or entire image cubes in both forward (radiance) as well as backward (reflectance) computation modes. An overview of this procedure is shown in Figure 1 for the retrieval of surface reflectance from AVIRIS data as presented in this paper.

3.2 LUT Computations

In order to generate the LUT, a selected RT code is run for two different flat reflectance spectra ($\rho_1 = 5\%$, $\rho_2 = 60\%$), for a single value or a range of atmospheric water vapour contents (U_{H_2O}), optical depths (δ_a), and terrain elevations (z) covering the prevailing atmospheric conditions and the terrain variation. These calculations made on the RT code's wavelength grid (λ_m) are performed at different pixel locations (x) to capture the sensor geometry. Accordingly, a LUT is generated with the following six dimensions:

LUT ($\lambda_m, \rho, x, z, U_{H_2O}, \delta_a$).

The LUTs for both AVIRIS scenes were set up as follows:

LUT ($\lambda_m = 1 \text{ cm}^{-1}$ wavelength grid (RT code selected: MODTRAN 2),

ρ_1 and ρ_2 ,

x : 3 pixel positions (two extreme viewing angles ($\pm 15^\circ$), nadir),

z : 3 terrain elevations (one low and high value to cover range, one in between),

U_{H_2O} : 3 water vapour values (one low and high value to cover range, one in between),

δ_a : 1 optical depth).

Accordingly, there are 54 MODTRAN2 runs necessary to generate this LUT, each run taking approximately 7 minutes on a Sun Microsystems SPARC 10/51. This leads to a total computation time of about 6.3 hours. Although the time is quite long, it is much less than running the RT code on a pixel-by-pixel basis. However, the time can be drastically decreased to about 2 minutes if the M5S code (20 cm^{-1} wavelength grid) is used in this LUT configuration. (It should be noted that the performance of MODTRAN2 is superior especially in the gas absorption regions (Staenz et al., 1994)). The input parameters for the MODTRAN2 runs are summarized in Table 1.

The resulting target radiances at the sensor ($L_{g_1}^*, L_{g_2}^*$) and the path radiances, ($L_{p_1}^*, L_{p_2}^*$) derived from the MODTRAN2 code were then scaled by the spectral ratio of the Green and Gao (1993) E_o function to that which is used in MODTRAN2 (Staenz et al., 1995). Other E_o data sets presently available are those implemented in M5S (Iqbal., 1983), 6S (Vermote et al., 1994), MODTRAN2 (Berk et al., 1989) and MODTRAN3 (Anderson et al., 1994). The next step involved the convolution of the model output radiances with the AVIRIS specific radiance using the relative spectral response profiles for the sensor's spectral bands.

Before converting the AVIRIS radiances into surface reflectances, the LUT was used to estimate the atmospheric water vapour content on a pixel-by-pixel basis from the image data themselves. A non-linear least square-fitting technique similar to those reported by Green et al. (1993) and Gao and Goetz (1990) was applied to the wavelength region covering both the 940 nm and 1030 nm absorption features. Results are shown in Figure 2 for scene 1. It can be seen that the distribution of the water vapour map follows the DEM.

3.3 Surface Reflectance Computation

The LUT was then interpolated to compute the parameters necessary for a conversion of the AVIRIS radiance into the surface reflectance on a pixel-by-pixel basis. The relationship between the reflectance ρ and the MODTRAN2 output radiances L_g^* and L_p^* can be written as (Williams et al., 1992):

$$L_{xi}^* = A \frac{\rho_i}{1 - \rho_i S} \quad (1)$$

and

$$L_{pi}^* = B \frac{\rho_i}{1 - \rho_i S} + L_a^* \quad , \quad (2)$$

where $i = 1, 2$, L_a^* is the radiance backscattered by the atmosphere, S is the spherical albedo of the atmosphere, and A and B are coefficients depending on geometric and atmospheric conditions. These equations can be solved for the unknowns A , B , L_a^* and S for each set of $(\rho_i, L_{gi}^*, L_{pi}^*)$. L_{gi}^* and L_{pi}^* are adjusted for the sensor's viewing condition, atmospheric water vapour content, and terrain elevation on a pixel basis for each spectral band.

Since the radiance (L^*) measured by AVIRIS is the sum of equations (1) and (2), the surface reflectance can be calculated as follows:

$$\rho = \frac{L^* - L_a^*}{A + B + S (L^* - L_a^*)} \quad . \quad (3)$$

This equation is valid for homogeneous areas, that is if the reflectance of the target in question is the same as the surrounding target reflectance ρ_e . For inhomogeneous areas ($\rho \neq \rho_e$), ρ_e needs to be incorporated into equation (3) by substituting ρ by ρ_e in equation (2) as well as in the denominator of equation (1).

Comparisons of surface reflectances retrieved with the LUT-based procedure and true MODTRAN2 runs show a relative error of $\pm 1\%$ in the AVIRIS wavelength region.

Figure 3 portrays retrieved surface reflectance spectra of vegetation (conifers, clear cut area, and alpine meadow) extracted from scene 1 using equation (3). An artificial target, asphalt, extracted from scene 2 is shown in Figure 4. Since this target is entirely surrounded by forested areas ($\rho \neq \rho_e$), the adjacency effect caused by this surrounding target was removed (dotted versus dashed curve). It can be seen that this effect is important for wavelengths below 700 nm.

4. CONCLUSIONS

Surface reflectance retrieval from AVIRIS data is presented in this paper. Good results were achieved with the linear LUT-based procedure using MODTRAN2 in combination with the Green and Gao E_o function. For this purpose, a six-dimensional LUT was generated with wavelength, surface reflectance, pixel location, terrain elevation, atmospheric water vapour content, and aerosol optical depth as the dimensions. This procedure has the advantage of using a RT code only for the generation of the LUT, and not on a pixel-by-pixel basis and, therefore, saves computation time. Despite the fact that the RT code is only run for a specific LUT configuration and the linearity of the approach, the retrieved surface reflectances are comparable with results from true RT code runs. Surface reflectance results in the AVIRIS wavelength regions indicate a relative error of $\pm 1\%$ using MODTRAN2. This procedure is implemented on the Imaging Spectrometer Analysis System (ISDAS), which runs on Sun Microsystems SPARC-10 workstations.

5. ACKNOWLEDGMENTS

The authors are grateful to P.M. Teillet, J.-C. Deguise, and J.-F. Guay of the Canada Centre for Remote Sensing and to J. Cheriyan and M. Budd of MacDonald Dettwiler and Associates for valuable discussions and technical support. Thanks are also due to C. Burke for excellent word processing of this paper.

6. REFERENCES

Anderson G.P., J. Wong, and J.H. Chetwynd, 1995, "MODTRAN3: An Update on Recent Validations Against Airborne High Resolution Interferometer Measurements," Summaries of the Fifth Annual JPL Airborne Earth Science Workshop, JPL Publication 95-1, vol. 1, Pasadena, California, pp. 5-8.

Berk, A., L.S. Bernstein, and D.C. Robertson, 1989, "MODTRAN: A Moderate Resolution Model of LOWTRAN7," Final Report, GL-TR-0122, AFGL, Hanscom AFB, Maryland, 42 pages.

Carrère, V., and J.E. Conel, 1992, "Validation of Atmospheric Correction of Airborne Visible/Infrared Imaging Spectrometer (AVIRIS) Radiance Data Based on Radiative Transfer Modeling," Proceedings of the International Symposium on Spectral Sensing Research, vol. 1, pp. 474-487.

Gao, B.-C., and A. F. H. Goetz, 1990, "Column Atmospheric Water Vapour and Vegetation Liquid Water Retrievals From Airborne Imaging Spectrometer Data," Journal of Geophysical Research, vol. 95, no. D4, pp. 3549-3564.

Gao, B.-C., K.B. Heidebrecht, and A.F.H. Goetz, 1993, "Derivation of Scaled Surface Reflectances from AVIRIS Data," Remote Sensing of Environment, vol. 44, pp. 165-178.

Green, R.O., and B.-C. Gao, 1993, "A Proposed Update to the Solar Irradiance Spectrum Used in LOWTRAN and MODTRAN," Summaries of the Fourth Annual JPL Airborne Geoscience Workshop, JPL Publication 93-26, vol. 1, Pasadena California, pp. 81-84.

Green, R.O., J.E. Conel, and D.A. Roberts, 1993 "Estimation of Aerosol Optical Depth and Additional Atmospheric Parameters for the Calculation of Apparent Reflectance From Radiance Measured by the Airborne Visible/Infrared Imaging Spectrometer," Summaries of the Fourth Annual JPL Airborne Geoscience Workshop, JPL Publication 93-26, vol. 1, Pasadena, California, pp. 73-76.

Iqbal., M., 1983, An Introduction to Solar Radiation, Academic Press, New York, 390 pages.

Kneizys, F.X., E.P. Shettle, L.W. Abreu, J.H. Chetwynd, G.P. Anderson, W.O. Gallery, J.E. Selby, and S.A. Clough, 1988, "User's Guide to LOWTRAN7," AFGL-TR-88-0177, Environmental Research Papers, No. 1010, Air Force Geophysics Laboratory, Hanscom AFB, Bedford, Maryland, 137 pages.

Staenz, K., D.J. Williams, G. Fedosejevs, and P.M. Teillet, 1994, "Surface Reflectance Retrieval from Imaging Spectrometer Data Using Three Atmospheric Codes," Proceedings of SPIE's International Symposium on Recent Advances in Remote Sensing and Hyperspectral Remote Sensing, vol. 2318, Rome, Italy, pp. 17-28.

Staenz, K., D.J. Williams, G. Fedosejevs, and P.M. Teillet, 1995, "Impact of Differences in the Solar Irradiance Spectrum on Surface Reflectance Retrieval with Different Radiative Transfer Codes", Summaries of the Fifth Annual JPL Airborne Earth Sciences Workshop, JPL Publications 95-1, vol. 1, Pasadena, California, pp.153-156.

Staenz, K., B. Walker, and J. Schwarz, 1996, "An Image Analysis System Designed for Information Extraction from Hyperspectral Data," Proceedings of the XVIII International Congress for Photogrammetry and Remote Sensing, Vienna, Austria (in preparation).

Tanré, D., C. Deroo, P. Duhaut, M. Herman, J.J. Morcrette, J. Perbos, and P.Y. Deschamps, 1990, "Description of a Computer Code to Simulate the Satellite Signal in the Solar Spectrum: The 5S Code," International Journal of Remote Sensing, vol. 11, no. 4, pp. 659-668.

Teillet, P.M., and R.P. Santer, 1991, "Terrain Elevation and Sensor Altitude Dependence in a Semi-Analytical Atmospheric Code," Canadian Journal of Remote Sensing, vol. 17, no. 1, pp. 36-44.

Vermote, E., D. Tanré, J. L. Deuzé, M. Herman, and J. J. Morcrette, 1994, "Second Simulation of the Satellite Signal in the Solar Spectrum (6S)", 6S User's Guide Version 6.0, NASA-GSFC, Greenbelt, Maryland, 134 pages.

Williams, D.J., A. Royer, N.T. O'Neill, S. Achal, and G. Weale, 1992, "Reflectance Extraction From CASI Spectra Using Radiative Transfer Simulations and a Rooftop Radiance Collector", Canadian Journal of Remote Sensing, vol. 18, no. 4, pp. 251-261.

Table 1. Input Parameters for the MODTRAN2 Runs

Parameter	Scene 1	Scene 2
Atmospheric model	Mid-latitude summer	Mid-latitude summer
Aerosol model	Continental	Continental
Date of overflight	August 2, 1990	August 29, 1993
Solar zenith angle	35.9°	46.9°
Solar azimuth angle	179°	218°
Sensor zenith angle	variable	variable
Sensor azimuth angle	variable	variable
Terrain elevation	variable	variable
Sensor altitude above sea level	19.850 km	19.360 km
Water vapour content	variable	variable
Horizontal visibility or Aerosol optical depth	50 km -	- 0.121 (measured)

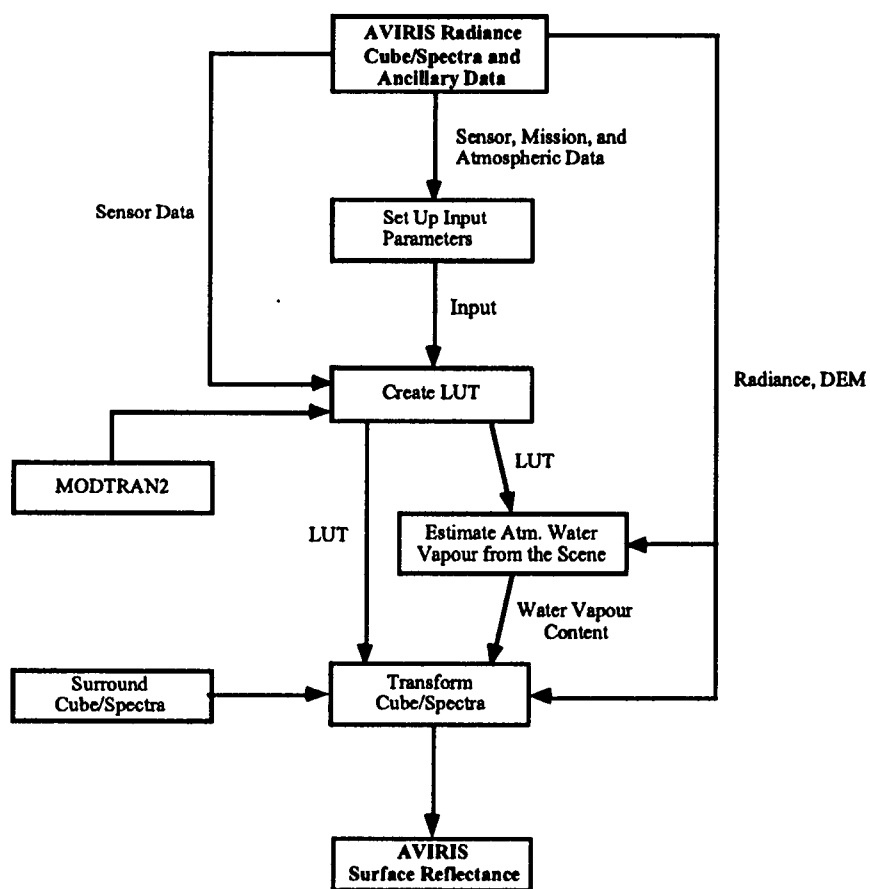


Figure 1: Layout of the LUT-based procedure for retrieval of surface reflectance from AVIRIS data.

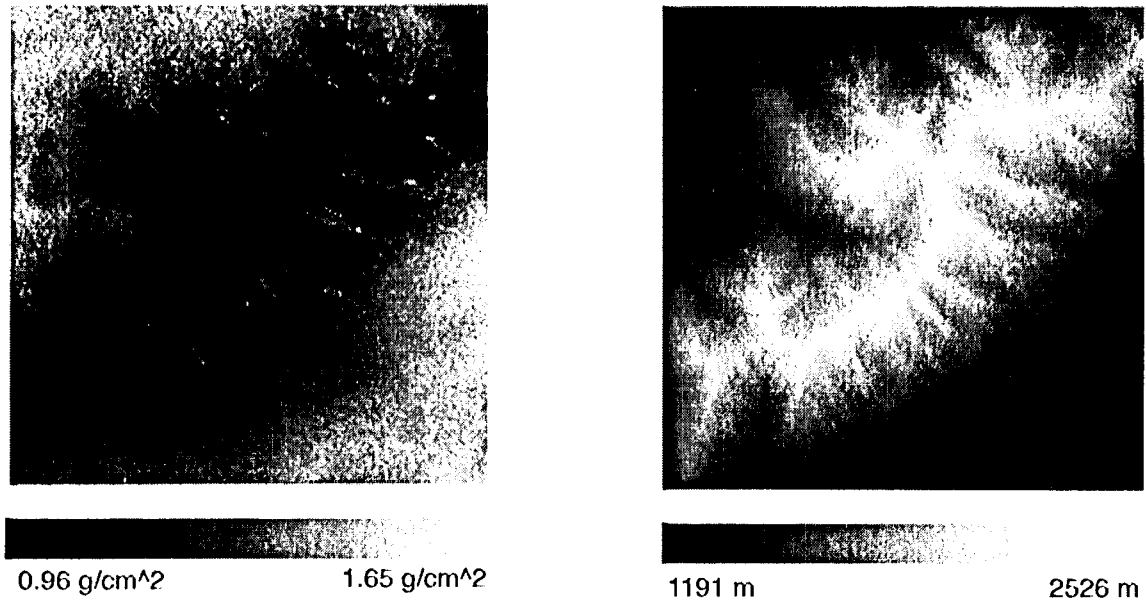


Figure 2: Distribution of the atmospheric water vapour content (left) extracted from AVIRIS scene 1. The DEM is shown on the right for the same area as a comparison.

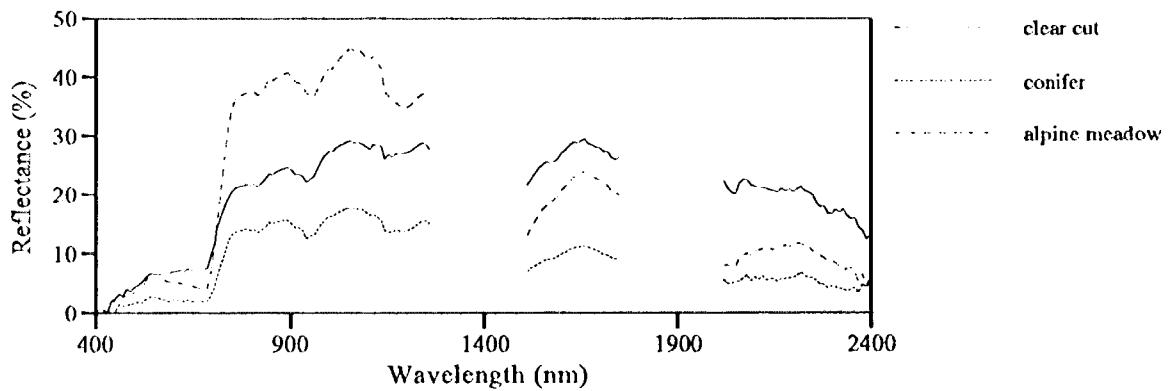


Figure 3: Surface reflectance spectra of different vegetation targets retrieved with the IUT-based approach using MODTRAN2 and the Green and Gao E_o function. Data are extracted from AVIRIS scene 1.

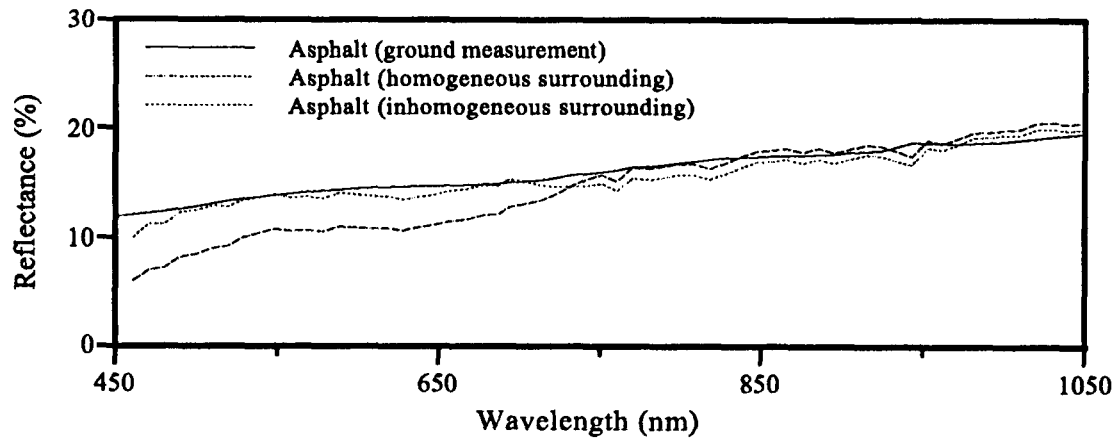


Figure 4: Surface reflectance spectra of asphalt retrieved from AVIRIS scene 2 and from ground-based measurements (solid curve) acquired with a MARK V spectroradiometer. The dashed and dotted curves represent data with homogeneous ($\rho = \rho_e$) and inhomogeneous surrounding terrain ($\rho \neq \rho_e$), respectively. ρ is the reflectance of the target in question and ρ_e is the reflectance of the surrounding targets.